

This is a pre print version of the following article:

Veering of Rayleigh–Lamb waves in orthorhombic materials / Nobili, A.; Erbas, B.; Signorini, C.. - In: MATHEMATICS AND MECHANICS OF SOLIDS. - ISSN 1081-2865. - 27:9(2022), pp. 1783-1799. [10.1177/10812865211073467]

*Terms of use:*

The terms and conditions for the reuse of this version of the manuscript are specified in the publishing policy. For all terms of use and more information see the publisher's website.

03/05/2026 13:59

(Article begins on next page)

---

# Veering of Rayleigh-Lamb waves in orthorhombic materials

Journal Title  
XX(X):2-26  
©The Author(s) 0000  
Reprints and permission:  
sagepub.co.uk/journalsPermissions.nav  
DOI: 10.1177/ToBeAssigned  
www.sagepub.com/

SAGE

A. Nobili<sup>1</sup>, B. Erbas<sup>2</sup> and C. Signorini<sup>3</sup>

## Abstract

We analyse veering of Rayleigh-Lamb waves in a thin orthotropic plate. We demonstrate that veering results from interference of partial waves in a similar manner as it occurs in systems composed of 1D structures, such as beams or strings. Indeed, in the neighbourhood of a veering point, the system may be approximated by a pair of interacting taut strings whose wave speed is the geometric average of the phase and group velocity of the relevant partial wave at the veering point. This complementary pair of partial waves provides the coupling terms in a form compatible with an action-reaction principle. We prove that veering of symmetric waves near the longitudinal bulk wave speed repeats itself indefinitely with the same structure. However, the dispersion behaviour of Rayleigh-Lamb waves is richer than that of 1D systems and this reflects also on the veering pattern. In fact, the interacting taut string model fails whenever the dispersion branch is not guided by either partial wave. This often occurs when neighbouring veering points interact and partial waves no longer provide guiding curves.

## Keywords

Veering, Rayleigh-Lamb waves, Orthorhombic elastic materials

## 1 Introduction

2 Rayleigh-Lamb (RL) waves in thin plates have long attracted great attention  
3 in view of their theoretical and practical importance. They encompass a large  
4 array of important phenomena such as dispersion, localization and interference.  
5 Despite their apparent simplicity, a satisfactory understanding of the underlying  
6 physics has only been gained in fairly recent times [4]. This understanding is  
7 especially valuable because it provides, among many assets, the foundation for  
8 consistent asymptotic reduced theories for shell, plates and beams [8, 14, 19, 11].  
9 Consideration of anisotropic features adds considerable complications and yet  
10 it possesses relevant practical importance, as well illustrated in the classical  
11 monograph [2]. As an example of such complications, following [20] we mention  
12 that Kirchhoff-Love and Timoshenko-Reissner plate models fail to be consistent  
13 with the outcomes of the 3D theory for a strongly orthotropic material. The  
14 recent review paper [9] accounts for the many contributions appearing in the  
15 literature that investigate specific features of RL propagation. For example, in  
16 [5] it is pointed out that orthotropy is attached to special points possessing zero-  
17 group velocity, which pave the way to anomalous dispersion, i.e. situations where  
18 the energy flows in the direction opposite to that of propagation for the wave  
19 train. Equally, [21] illustrate the effect of curvature on the waveguide properties.

20 Wave coupling occurs in multiple instances, such as in reduced models, e.g.  
21 strings, beams and rods [18, 7] or between different propagation modes, as it  
22 is the case for torsional and bending waves [3]. Coupling of waves takes up  
23 many different forms (for instance through mode conversion and localization  
24 [13]), among which veering is especially remarkable, because it is associated  
25 with rapid divergence of the propagation branches in the neighbourhood of the  
26 veering point, alongside eigenvector inversion. This peculiar behaviour may be  
27 most easily explained in coupled oscillators, where tuning the coupling device  
28 brings the specific propagation features of either in a veering condition. In [10, 1],

---

<sup>1</sup> University of Modena and Reggio Emilia, Department of Engineering Enzo Ferrari, via Vivarelli 10, 41125 Modena, Italy

<sup>2</sup> Eskisehir Technical University, Department of Mathematics, Yunus Emre Campus, 26470, Eskisehir, Turkey

<sup>3</sup> Technical University Dresden, Institute of Construction Materials, Georg-Schumann-Str. 7, 01187 Dresden, Germany

**Corresponding author:**

Andrea Nobili, Department of Engineering Enzo Ferrari, via Vivarelli 10, 41125 Modena, Italy  
Email: andrea.nobili@unimore.it

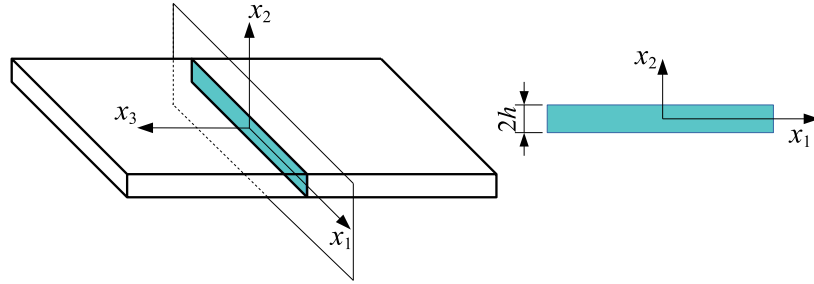


**Figure 1.** A free infinite orthotropic thin plate in plane strain

29 Manconi and Mace study veering in discrete conservative elastic systems under  
 30 a framework for the analysis thereof. They distinguish between weak and strong  
 31 coupling and introduce the concept of uncoupled block system.

32 In this paper, we investigate veering in a continuous system, namely for RL  
 33 waves. In this situation, matter is complicated by the presence of multiple wave  
 34 modes (branches) and internal coupling. Nonetheless, we can show that the  
 35 concept of partial waves still work as a building block for both the dispersion  
 36 pattern and the interference thereof. After developing the classical governing  
 37 equations and travelling wave solution for orthorhombic media, respectively in  
 38 Sec. and , partial waves are introduced and analysed in Sec.. In Sec., they are  
 39 shown to guide RL modes and their intersection defines the veering points and  
 40 the form of the interacting systems (Sec.). Finally, conclusions are drawn in  
 41 Sec..

## 42 Governing equations

43 Let us consider an infinite thin plate of thickness  $2h$ , made of linear elastic  
 44 homogeneous material with orthorhombic material symmetry (Fig.1). The strip  
 45 lower/upper boundaries are located, respectively, at  $x_2 = \pm h$ . We consider the  
 46 situation when  $x_3$  is a direct axis of even order (i.e. the plane  $(x_1, x_2)$  is a  
 47 mirror plane) and  $x_1$  is directed along a symmetry axis for the material, as in  
 48 [15]. For convenience, Voigt's (or matrix) notation is adopted throughout [16,  
 49 p.134], according to which

$$(11) \leftrightarrow 1, (22) \leftrightarrow 2, (33) \leftrightarrow 3, (23) = (32) \leftrightarrow 4, (13) = (31) \leftrightarrow 5, (12) = (21) \leftrightarrow 6.$$

50 Therefore, as an example,  $c_{11} = c_{1111}$ ,  $c_{12} = c_{1122} = c_{2211}$  and  $c_{66} = c_{1212} =$   
 51  $c_{2112} = c_{2121} = c_{1221}$ . The elastic constants are gathered in the stiffness matrix  
 52 [15, Eq.(3.64)]

$$\mathbf{C} = \begin{bmatrix} c_{11} & c_{12} & c_{13} & 0 & 0 & 0 \\ c_{12} & c_{22} & c_{23} & 0 & 0 & 0 \\ c_{13} & c_{23} & c_{33} & 0 & 0 & 0 \\ 0 & 0 & 0 & c_{44} & 0 & 0 \\ 0 & 0 & 0 & 0 & c_{55} & 0 \\ 0 & 0 & 0 & 0 & 0 & c_{66} \end{bmatrix}. \quad (1)$$

53 It is important to emphasize that  $\mathbf{C}$  is not a rank-2 tensor, for it lacks the  
 54 transformation property thereof. The off-diagonal coefficients  $c_{12}$ ,  $c_{13}$  and  $c_{23}$  are  
 55 sometimes referred to as coupling stiffnesses and they may be positive, negative  
 56 or zero. Cubic symmetry, that is considered in [17], may be retrieved upon  
 57 taking  $c_{12} = c_{13} = c_{23}$ ,  $c_{11} = c_{22} = c_{33}$  and  $c_{44} = c_{55} = c_{66}$ . Isotropic materials  
 58 are a special case of cubic symmetry with

$$c_{11} = \lambda + 2\mu, \quad c_{12} = \lambda, \quad c_{66} = \mu, \quad (2)$$

59 where  $\mu > 0$  and  $\lambda > -\frac{2}{3}\mu$  are Lamé elastic constants. The plane  $(x_1, x_2)$   
 60 is named the *sagittal plane of wave propagation*, because it contains the  
 61 surface normal and the propagation direction (wave vector) [16, §5.1]. Under  
 62 such conditions, it is well known that the Christoffel matrix governing wave  
 63 propagation has block form and the corresponding linear system breaks up into  
 64 two independent subsystems: one accounting for longitudinal (P) and shear  
 65 vertical (SV) propagation (for such motions the polarization vector lies in the  
 66 sagittal plane) and the other for shear horizontal (SH) propagation, see [16,  
 67 §5.1.1(a)] and [17]. We recall that positiveness of the strain energy density  
 68 demands

$$c_{11}, c_{22}, c_{66} > 0, \quad c_{11}c_{22} - c_{12}^2 > 0, \quad (3)$$

69 so thus we may define the generalized Young modulus

$$E_c = c_{11} - \frac{c_{12}^2}{c_{22}}.$$

70 It should be emphasized that  $E_c$  may be written in terms of the technical (or  
 71 engineering) moduli [6]

$$E_c = \frac{E_1}{1 - \nu_{13}\nu_{31}},$$

and, in an isotropic material, it reduces to the Young modulus in plane strain  $E_c = E/(1 - \nu^2)$ . We note that, in an anisotropic plate, the bending stiffness within the Kirchhoff theory is given by  $D_x = E_c I$  and  $D_y = \nu_{31} D_x / \nu_{13}$ , wherein  $I = 2h^3/3$  is the second moment of inertia, see, for example, [14].

In an orthorhombic material, several bulk wave speeds are defined, see [16],

$$c_1 = \sqrt{\frac{c_{11}}{\rho}}, \quad c_2 = \sqrt{\frac{c_{22}}{\rho}}, \quad c_{SV} = \sqrt{\frac{c_{66}}{\rho}}, \quad c_{SH} = \sqrt{\frac{c_{55}}{\rho}}, \quad (4)$$

respectively bulk longitudinal along  $x_1$  and along  $x_2$  and transverse shear vertical (SV) and shear horizontal (SH) wave speed. To such speeds, in analogy to the longitudinal wave speed for beams, we add the combination [12]

$$c_c = \sqrt{\frac{E_c}{\rho}} < c_1. \quad (5)$$

Strain  $\epsilon$  is small and it is related to the displacement field  $\mathbf{u} = [u_1, u_2, u_3]$  through the linear relations

$$\epsilon_{ij} = \frac{1}{2}(u_{i,j} + u_{j,i}), \quad i, j \in \{1, 2, 3\},$$

where a suffix comma denotes differentiation with respect to the relevant space variable, e.g.  $u_{1,1} = \partial u_1 / \partial x_1$ , and summation over twice repeated subscripts is assumed. We recall that  $\gamma_{ij} = 2\epsilon_{ij}$ ,  $i \neq j$  is the engineering shear strain. The stress  $\boldsymbol{\sigma}$  is related to strain through Hook's constitutive law

$$\boldsymbol{\sigma} = \mathbf{C}\boldsymbol{\epsilon}. \quad (6)$$

The equilibrium equations, in the absence of body forces, read

$$\sigma_{ij,j} = \rho \ddot{u}_i,$$

and they take on the expanded form (superposed dots denote time differentiation) valid for orthorhombic materials

$$c_{11}u_{1,11} + c_{55}u_{1,33} + c_{66}u_{1,22} + (c_{12} + c_{66})u_{2,12} + (c_{13} + c_{55})u_{3,13} = \rho \ddot{u}_1, \quad (7a)$$

$$c_{66}u_{2,11} + c_{44}u_{2,33} + c_{22}u_{2,22} + (c_{12} + c_{66})u_{1,12} + (c_{23} + c_{44})u_{3,23} = \rho \ddot{u}_2, \quad (7b)$$

$$c_{55}u_{3,11} + c_{44}u_{3,22} + c_{33}u_{3,33} + (c_{13} + c_{55})u_{1,13} + (c_{23} + c_{44})u_{2,23} = \rho \ddot{u}_3. \quad (7c)$$

## 86 Waves in unbounded media

87 Christoffel equations are obtained plugged into the equilibrium equations (7)  
88 travelling wave solutions in the form

$$u_i(x_1, x_2, x_3, t) = A_i \exp[\iota(k_1 x_1 + k_2 x_2 + k_3 x_3 - \omega t)], \quad (8)$$

89 where  $\mathbf{A} = [A_i]$  is the polarization vector,  $\mathbf{k} = [k_i]$  the wave vector,  $\omega$  the wave  
90 frequency and  $\iota$  the imaginary unit, i.e.  $\iota^2 = -1$ . Since we restrict attention  
91 to waves propagating in the sagittal plane  $(x_1, x_2)$ , we have  $k_3 = 0$  and no  
92 dependence on  $x_3$  (i.e. plane strain). We introduce the ratio  $\Lambda = k_2/k_1$ , which  
93 corresponds to the tangent of the angle of wave propagation to the  $x_1$ -axis.

94 The general solution of the Rayleigh-Lamb dispersion problem may be  
95 constructed from a superposition of simple waves, named *partial waves* [4, 17].  
96 Partial waves travel along the plate (along  $x_1$ ) with the same wavenumber  
97  $k_1 = k > 0$ , while bouncing back and forth at the plate boundaries. Their  
98 interaction is generally induced by the boundary conditions and determine the  
99 dispersion pattern. Here,  $v = \omega/k$  is the phase velocity along  $x_1$ .

100 The determination of the wave vector (eigenvalues) for the Christoffel  
101 equations leads to a sixth degree real-coefficient polynomial equation in  $\lambda$ , which  
102 may be factored into the product of a second degree polynomial, governing  
103 SH waves for which  $\mathbf{A} = [0, 0, 1]$ , with a fourth degree polynomial, governing  
104 partial waves polarized in the sagittal plane, i.e.  $\mathbf{A} = [A_1, A_2, 0]$ . Indeed, the  
105 corresponding eigenvectors correspond to the wave polarization.

106 In order to determine the wave vectors we introduce the dimensionless space  
107 and time co-ordinates

$$\{\xi_1, \xi_2, \tau\} = \{h^{-1}x_1, h^{-1}x_2, T^{-1}t\}, \quad (9)$$

having let the reference time  $T$  in terms of the body shear wave speed  $c_{SV}$

$$T = \frac{h}{c_{SV}}.$$

In this framework, we define the dimensionless velocities

$$V_1 = c_1/c_{SV}, \quad V_2 = c_2/c_{SV}, \quad V_5 = c_{SH}/c_{SV}, \quad V_c = c_c/c_{SV} < V_1.$$

From now on, with a slight abuse of notation, a subscript comma indicates partial differentiation with respect to the relevant dimensionless variables, i.e.  $u_{3,1} = \partial u_3 / \partial \xi_1$ . Besides, for the sake of compactness, we may sometimes drop the explicit indication of functional dependence, e.g. we may write  $u_i$  instead of  $u_i(\xi_1, \xi_2, \tau)$ . The equilibrium equations for plane motions (7) become (cfr.[5])

$$\frac{c_{11}}{c_{66}} u_{1,11} + u_{1,22} + \left( \frac{c_{12}}{c_{66}} + 1 \right) u_{2,12} = u_{1,\tau\tau}, \quad (10a)$$

$$u_{2,11} + \frac{c_{22}}{c_{66}} u_{2,22} + \left( \frac{c_{12}}{c_{66}} + 1 \right) u_{1,12} = u_{2,\tau\tau}, \quad (10b)$$

108 while antiplane motion is governed by

$$\frac{c_{55}}{c_{66}} u_{3,11} + \frac{c_{44}}{c_{66}} u_{3,22} = u_{3,\tau\tau}. \quad (11)$$

We shall look for solutions in the form of plane harmonic waves

$$u_i(\xi_1, \xi_2, \tau) = U_i(\xi_2) \exp i(K\xi_1 - \Omega\tau), \quad i \in \{1, 2, 3\},$$

109 where  $K = k_1 h$  and  $\Omega = \omega T > 0$  are the dimensionless wavenumber and angular  
110 frequency. With these definitions,  $V = \Omega/K = v/c_{SV}$ . Antiplane motions give  
111 immediately the characteristic equation for  $\lambda_{SH}$

$$\lambda_{SH}^2 = \frac{c_{66}}{c_{44}} K^2 (V_5^2 - V^2), \quad (12)$$

112 whence we can write the general solution

$$U_3(\xi_2) = a_1 \lambda_{SH}^{-1} \sinh(\lambda_{SH} \xi_2) + a_2 \cosh(\lambda_{SH} \xi_2), \quad (13)$$

113 where  $a_1$  and  $a_2$  are arbitrary constants and the solution has been written in a  
114 form independent of the sign chosen for  $\lambda_{SH}$ .

The equilibrium equations for the in-plane motion (10) may be cast in terms of a single fourth order ODE in either  $U_1(\xi_2)$  or  $U_2(\xi_2)$ , say

$$a_2 U_1''''(\xi_2) + a_1 U_1''(\xi_2) + a_0 U_1(\xi_2) = 0,$$

115 which lends the bi-quadratic characteristic equation for  $\lambda$

$$a_2 \lambda^4 - a_1 K^2 \lambda^2 + a_0 K^4 = 0, \quad (14)$$

where (cfr.[12] with  $c_{66}V^2 = \rho c_R^2$ )

$$\begin{aligned} a_2 &= c_{22}c_{66}, \\ a_1 &= c_{11}c_{22} \left(1 - \frac{V^2}{V_1^2}\right) + c_{66}^2(1 - V^2) - (c_{12} + c_{66})^2 \\ a_0 &= c_{11}c_{66} (1 - V^2) \left(1 - \frac{V^2}{V_1^2}\right). \end{aligned}$$

116 The coefficient  $a_1$  is the generalization to orthorhombic materials of the  
117 coefficient  $B$  of [17]. Clearly, the sign of  $\lambda$  is immaterial and therefore, without  
118 loss of generality, we restrict attention to the pair of solutions of Eq.(14) with  
119 positive real part

$$\lambda_{1,2} = K\Lambda_{1,2}, \quad \Re(\Lambda_{1,2}) \geq 0, \quad (15)$$

120 being

$$\Lambda_{1,2}^2 = \frac{a_1 \mp \sqrt{\Delta}}{2a_2}, \quad \Delta = a_1^2 - 4a_0a_2. \quad (16)$$

121 With this restriction, a branch cut for the square root is selected. With  
122 such definitions,  $\Lambda_{1,2} = \Lambda_{1,2}(V^2)$  are functions of the phase velocity squared  
123  $V^2$ . Physically,  $\Lambda_{1,2}$  represent the ratio between longitudinal and transversal  
124 wavenumbers, i.e.  $\tan \beta$ , where  $\beta$  is the angle of wave propagation to the  $x$ -  
125 axis. In particular, whenever  $\Lambda_{1,2} = 0$  an infinite plane wave-front propagating  
126 indefinitely is possible, that is a bulk wave. In the isotropic case, we have  
127 that the discriminant  $\Delta = \mu^2(\lambda + \mu)^2 K^2 V^2$  is always positive and, as expected,  
128  $\Lambda_{1,2}(0) = 1$  for standing waves propagate equally in either direction. When  
129  $\Delta < 0$ ,  $\Lambda_{1,2}^2$  becomes a complex conjugated pair describing evanescent waves.  
130 The expressions for  $\lambda_{1,2}$  represent a generalization to orthothropic materials of  
131 Eq.(17) of [17]. Similarly to there, the smallest solution (in terms of absolute  
132 value) of (16) corresponds to quasi-longitudinal waves (QP), while the largest  
133 gives quasi-shear waves (QSV)\*. We observe that Eq.(14) is also the secular  
134 equation for the attenuation index of Rayleigh waves, see [15, Eq.(10)] and [16,  
135 Eq.(5.54)], with  $a_1/a_2 = S$  and  $a_0/a_2 = P$ . For large values of  $V$  we get

$$\Lambda_1 = -V^2, \quad \Lambda_2 = -V^2/V_2^2. \quad (17)$$

---

\*In [17] reference is made to the minus and to the plus solutions, which however correspond to the smallest and to the largest only inasmuch as  $a_1 > 0$ .

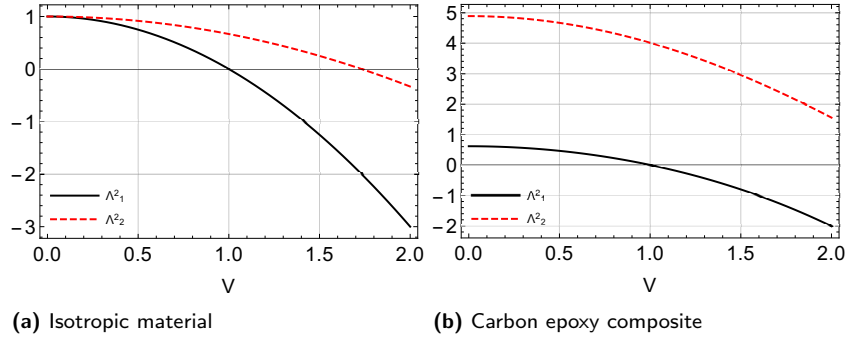


**Figure 2.**  $\Lambda_{1,2}$  vs.  $V$

136 It is expedient to introduce the auxiliary quantity

$$V_*^2 = (1 + V_2^{-2})^{-1} \left( V_c^2 - 2 \frac{c_{12}}{c_{22}} \right), \quad (18)$$

137 such that the sign of  $a_1$  may be easily determined from

$$a_1 = c_{66}^2 (1 + V_2^2) (V_*^2 - V^2).$$

138 We observe that, in general,  $V_*^2$  may be positive, negative or zero. Assuming  
139 the condition

$$c_{66} \leq \sqrt{c_{11}c_{22}} - c_{12}, \quad (19)$$

140 warrants that  $V_*^2 \geq 0$ . Besides, if  $c_{12} \geq 0$ , we have  $0 < V_*^2 < V_c^2 < V_1^2$  and  $a_1 \geq 0$   
141 provided that  $V^2 \leq V_*^2$ . In the isotropic case, the inequality (19) is strictly  
142 satisfied and we have

$$V_*^2 = 2 \left( 1 - \frac{1}{1 + V_1^2} \right). \quad (20)$$

143 We observe that, according to Eq.(20), we have  $1 < V_* < V_1$ . With the usual  
144 restriction on the Lamé constants, it is further seen that  $2\sqrt{2/7} < V_* < \sqrt{2}$ .  
145 Hereinafter, to fix ideas, we shall assume that

$$1 < V_* < V_c < V_1 \quad (21)$$

146 holds also in the orthorhombic case, which is usually the case for real  
147 orthorhombic materials.

Speed	Steel	Carbon-epoxy
$V_*$	1.24	1.92
$V_c$	1.69	2.45
$V_1$	1.87	2.48
$V_2$	1.87	1.43
$V_R$	0.93	0.96

**Table 1.** Dimensionless wave speeds for steel (22) and carbon-epoxy (23)

148 In the following, when giving numerical results, we shall consider steel as a  
149 prototype for isotropic materials

$$\lambda = 115 \text{ GPa} \quad \mu = 77 \text{ GPa}, \quad (22)$$

150 and carbon-epoxy composite for orthorombic materials

$$c_{11} = 55.15 \text{ GPa}, \quad c_{22} = 18.38 \text{ GPa}, \quad c_{66} = 9.00 \text{ GPa}, \quad c_{12} = 4.60 \text{ GPa}. \quad (23)$$

151 Tab.1 gathers the dimensionless speeds for both materials. Fig.2 shows that  
152  $\Lambda_{1,2}^2$  are monotonic decreasing functions of  $V$  that are concave downwards,  
153 i.e.  $d^2\Lambda_{1,2}/dV^2 < 0$ . They possess the simple zero  $\Lambda_1^2(1) = \Lambda_2^2(V_1) = 0$  and,  
154 consequently,  $V = 1$  and  $V = V_1$  are branch points for the square root in  $\Lambda_{1,2}$ ,  
155 respectively. It follows that the relevant derivatives  $d\Lambda_1/dV(1)$  and  $d\Lambda_2/dV(V_1)$   
156 turn unbounded. Obviously,  $\Lambda_{1,2}$  are both real for  $V < 1$ , respectively purely  
157 imaginary and real for  $1 < V < V_1$  and both purely imaginary for  $V > V_1$ . For  
158 future purposes, we determine

$$\Lambda_1^2(V_1) = -(1 + V_2^{-2})(V_1^2 - V_*^2). \quad (24)$$

159 The solution of the equilibrium equations (10) is

$$\begin{bmatrix} U_1(\xi_2) \\ U_2(\xi_2) \end{bmatrix} = \mathbf{G}\boldsymbol{\varphi} \quad (25)$$

160 where  $\boldsymbol{\varphi} = [e_1, e_2, o_1, o_2]$  and

$$\mathbf{G} = \begin{bmatrix} \cosh(\lambda_1\xi_2) & \cosh(\lambda_2\xi_2) & \lambda_1^{-1}\sinh(\lambda_1\xi_2) & \lambda_2^{-1}\sinh(\lambda_2\xi_2) \\ i\alpha_1\sinh(\lambda_1\xi_2) & i\alpha_2\sinh(\lambda_2\xi_2) & i\lambda_1^{-1}\alpha_1\cosh(\lambda_1\xi_2) & i\lambda_2^{-1}\alpha_2\cosh(\lambda_2\xi_2) \end{bmatrix}.$$

161 The vector  $\varphi$  will be separated in the first and in the second pair of  
 162 components, namely  $\varphi = [\varphi_e, \varphi_o]$ . The matrix  $\mathbf{G}$  is arranged thus to show that  
 163 the displacement is indeed independent on the sign of the lambdas. In Eq.(25),  
 164 we have let the dimensionless functions of  $V^2$  (cfr.[12, Eq.(17)])

$$\alpha_{1,2}(V) = \frac{c_{66}}{c_{12} + c_{66}} \left( \Lambda_{1,2} + \frac{V^2 - V_1^2}{\Lambda_{1,2}} \right). \quad (26)$$

165 It is worth noticing that  $\alpha_1(V)$  blows up for  $V \rightarrow 1$ , for then  $\Lambda_1(V) \rightarrow 0$  as  
 166  $\sqrt{V-1}$ . Conversely, as  $V \rightarrow V_1$ , it is  $\Lambda_2(V_1) \rightarrow 0$  and yet  $\alpha_2(V_1) \rightarrow 0$ , while

$$\alpha_1(V_1) = \left( 1 + \frac{c_{12}}{c_{66}} \right)^{-1} \Lambda_1(V_1) \quad (27)$$

is purely imaginary in view of (24) and of the inequalities (21). We observe that  
 the Rayleigh function may be written in a symmetric form in terms of  $\alpha_i$  and  
 $\Lambda_i$ ,  $i \in \{1, 2\}$ , as [12]

$$R(V^2) = \begin{vmatrix} \imath\zeta_{11} & \imath\zeta_{12} \\ -\imath\zeta_{21} & -\imath\zeta_{22} \end{vmatrix} = s_1 - s_2,$$

having let

$$\begin{aligned} \zeta_{11}(V) &= 1 + \frac{c_{22}}{c_{12}} \alpha_1 \Lambda_1, & \zeta_{12}(V) &= 1 + \frac{c_{22}}{c_{12}} \alpha_2 \Lambda_2, \\ \zeta_{21}(V) &= \imath(\Lambda_1 - \alpha_1), & \zeta_{22}(V) &= \imath(\Lambda_2 - \alpha_2), \end{aligned}$$

and, clearly,

$$s_1 = \zeta_{11}\zeta_{22}, \quad s_2 = \zeta_{12}\zeta_{21}.$$

167 Therefore, we can determine the Rayleigh wave speed  $V_R$  as the single real  
 168 solution of the equation

$$s_1(V_R) - s_2(V_R) = 0. \quad (28)$$

## 169 Partial waves

170 Rayleigh-Lamb waves emerge from consideration of the plate boundary  
 171 conditions (BCs). In particular, when Mindlin's BCs are considered, either the  
 172 micro-chain (MC) conditions,

$$\sigma_{22} = 0 \quad \text{and} \quad u_1 = 0, \quad (29)$$

173 or the lubricated rigid support (LRS) conditions

$$\sigma_{12} = 0 \quad \text{and} \quad u_2 = 0, \quad (30)$$

Rayleigh-Lamb waves collapse into partial waves. In standard practice, symmetric and antisymmetric (flexural) Rayleigh-Lamb waves are discussed separately: they are obtained splitting the problem in its even and odd part with respect to  $\xi_2$ , see [4, 17]. This separation holds also for partial waves. For symmetric LRS and antisymmetric MC we have

$$(\alpha_2 \lambda_1 - \alpha_1 \lambda_2) \sinh \lambda_1 \sinh \lambda_2 = 0,$$

while for symmetric MC and antisymmetric LRS it is

$$(\alpha_2 \lambda_1 - \alpha_1 \lambda_2) \cosh \lambda_1 \cosh \lambda_2 = 0.$$

174 The first set of solutions satisfying either dispersion relation is

$$\lambda_2 = i \frac{1}{2} m \pi, \quad m \in \{0, 1, 2, \dots\}, \quad (31)$$

175 and it corresponds to a family of P modes. Therefore, P modes bounce back and  
 176 forth at the plate boundaries with an integer number,  $m$ , of half wavelengths  
 177 occurring in between. Accordingly, they appear in the same (opposite) fashion at  
 178 the plate boundaries, i.e. they are symmetric (antisymmetric), when  $m$  is even  
 179 (odd). Antisymmetric waves repeat periodically every two thickness cycles. In  
 180 particular, the P mode  $m = 0$  describes a plane wave with speed  $V = V_1$ , i.e. it  
 181 gives bulk longitudinal waves. Symmetric and antisymmetric P modes possess  
 182 the eigenforms  $\phi_{eP} = (0, 1)$  and  $\phi_{oP} = (0, 1)$ , respectively. Similarly, the second  
 183 set of solutions

$$\lambda_1 = i \frac{1}{2} n \pi, \quad n \in \{0, 1, 2, \dots\}, \quad (32)$$

184 provides a family of SV modes, which may equally be even or odd according to  
 185 the parity of  $n$ . Symmetric and antisymmetric SV modes possess the eigenforms  
 186  $\phi_{eSV} = (1, 0)$  and  $\phi_{oSV} = (1, 0)$ , respectively. In the terminology of [1], partial  
 187 waves describe the uncoupled-blocked systems and their spectra (31,32) form  
 188 the *skeleton of the eigenvalues*, wherein the wavenumber  $K$  acts as variable  
 189 parameter.

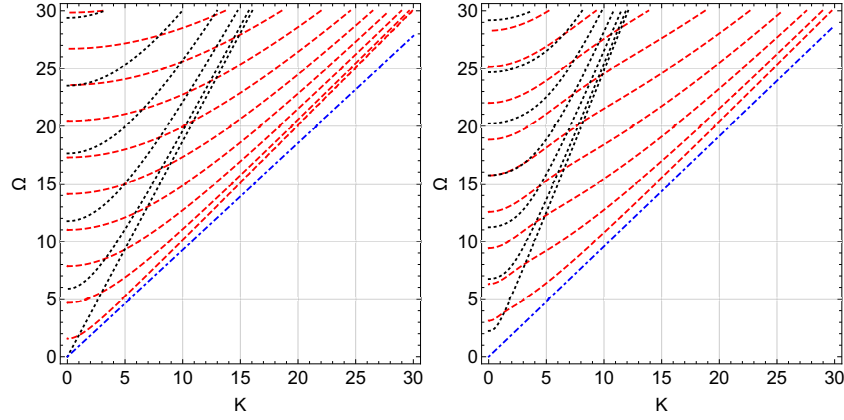


**Figure 3.** Partial waves for steel: even (odd) P modes (dotted, black) and odd (even) SV modes (dashed, red), respectively left and right panel. The Rayleigh wave line-spectrum is also shown (dash-dotted, blue)

190 The definition (15) together with Eqs.(31) and (32) show that P and SV  
 191 modes may be written as a function of  $K^2$  and  $V^2$ . The dimensionless group  
 192 velocity of such partial waves is given by

$$V_{g_{1,2}}(V) = \frac{d\Omega}{dK} = V - \frac{\Lambda_{1,2}}{d\Lambda_{1,2}/dV}(V) \quad (33)$$

193 wherein the last term is the reciprocal of the logarithmic derivative. In particular

$$V_{g_1}(1) = 1, \quad V_{g_1}(V_1) = V_1 \left( 1 - \frac{1 - V_*^2/V_1^2}{1 - \frac{V_2^2(V_1^2-1)}{(1+V_2^2)^2(V_1^2-V_*^2)}} \right) < V_1, \quad (34)$$

194 and clearly  $V_{g_2}(V_1) = V_1$ . In the isotropic case, it is  $V_{g_1}(V_1) = V_1^{-1}$ . In light of  
 195 the fact that  $\Lambda_{1,2}^2$  are decreasing functions of  $V$  and observing that Eq.(33) may  
 196 be rewritten as

$$V_{g_{1,2}}(V) = V - 2 \frac{\Lambda_{1,2}^2}{d\Lambda_{1,2}^2/dV},$$

197 it is easily proved that, for  $V < 1$ , we have  $V_g > V$ , that is waves move slower  
 198 than the wave packet as ripples in a pond. However, there are no partial wave  
 199 branches in that region. For  $1 < V < V_1$ , there are only SV wave branches  
 200 describing SV waves moving faster than the wave packet, i.e.  $V > V_{g_1}$ . Finally,  
 201 for  $V > V_1$ , both P and SV waves move faster than the wave packet.

202 P and SV modes frequency spectra for a steel plate are plotted in Fig.3. It  
 203 clearly appears that P modes with  $m \geq 1$  asymptote bulk longitudinal waves  
 204 from above and similarly SV modes asymptote bulk SV waves from above.  
 205 Indeed, writing  $\lambda_2 = K\Lambda_2$  and considering the limit  $K \rightarrow +\infty$  along any curve  
 206 (31), demands that  $\Lambda_2 \rightarrow i0$ , which in turn requires  $V \rightarrow V_1^+$ , for the product  
 207  $K\Lambda_2$  to yield a finite purely imaginary number. A similar argument shows that  
 208  $V \rightarrow 1^+$  in the limit  $K \rightarrow +\infty$  for SV modes (32).

## 209 Rayleigh-Lamb waves

For a free plate, we have the BCs

$$\sigma_{22} = \sigma_{12} = \sigma_{32} = 0, \quad \text{at } x_2 = \pm h,$$

210 that, introducing the constitutive law (6), become

$$\frac{c_{12}}{c_{66}}u_{1,1} + \frac{c_{22}}{c_{66}}u_{2,2} = 0, \quad u_{1,2} + u_{2,1} = 0, \quad \text{and} \quad u_{3,2} = 0, \quad \text{at } \xi_2 = \pm 1. \quad (35)$$

## 211 SH waves

212 As already pointed out, in orthorhombic materials SH waves are decoupled from  
 213 SV and P waves. Enforcing the last of the BCs (35) on the general solution (13)  
 214 lends the dispersion relation

$$\sinh(2\lambda_3) = 0,$$

215 whose solutions are

$$\lambda_3^2 = -p^2\pi^2/4, \quad p = \{1, 2, 3, \dots\}. \quad (36)$$

216 Besides, we have that  $a_1 = 0$  whence  $U_3(\xi_2)$  is an even function of  $\xi_2$ . The  
 217 frequency spectrum for SH waves is plotted in Fig.4. It is worth observing that,  
 218 for large values of  $K$ , the spectrum curves tend to the SH bulk wave velocity  
 219  $V = V_5$ .

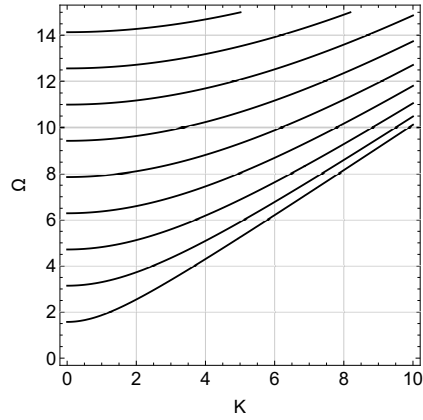


Figure 4. Frequency spectrum (36) for SH waves in a carbon epoxy plate

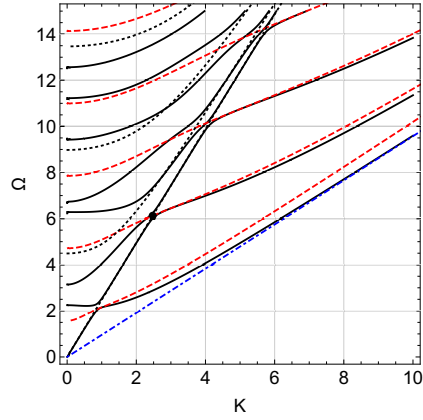


Figure 5. Frequency spectrum for symmetric waves in a free carbon epoxy-resin composite plate superposed onto even P (dotted, black) and odd SV (dashed, red) modes. A veering point (black dot) and the Rayleigh wave line spectrum (dash-dotted, blue) are also presented

## 220 *Symmetric waves*

221 Consideration of symmetric waves leads the homogeneous algebraic system

$$\mathbf{S}(K, \Omega) \begin{bmatrix} e_1 \\ e_2 \end{bmatrix} = \begin{bmatrix} 0 \\ 0 \end{bmatrix}, \quad (37)$$

where we have let the matrix

$$\mathbf{S}(K, \Omega) = \begin{bmatrix} \zeta_{11} \cosh \lambda_1 & \zeta_{12} \cosh \lambda_2 \\ -i\zeta_{21} \sinh \lambda_1 & -i\zeta_{22} \sinh \lambda_2 \end{bmatrix}.$$

222 This matrix may be rewritten in hermitian form

$$\mathbf{S}_h(K, \Omega) = \begin{bmatrix} i\zeta_{11}\zeta_{21}\frac{\cosh\lambda_1}{\cosh\lambda_2} & s_2 \\ -is_2 & -i\zeta_{12}\zeta_{22}\frac{\sinh\lambda_2}{\sinh\lambda_1} \end{bmatrix}. \quad (38)$$

Demanding that non-trivial solutions of the system (37) exist provides the dispersion relation (cfr.[4, Eq.(8.1.54)])

$$d_s(K^2, \Omega^2) = 0,$$

223 with

$$d_s(K^2, \Omega^2) = s_1 \coth \lambda_1 - s_2 \coth \lambda_2. \quad (39)$$

224 The frequency spectrum of a plate made of carbon-epoxy composite is plotted  
225 in Fig.5. We observe that odd SV modes are obtained through setting  $S_{11} = 0$   
226 and even P modes through putting  $S_{22} = 0$ , where  $S_{ij}$  denotes the  $(i, j)$ -element  
227 of the matrix  $\mathbf{S}$  of Eq.(37).

228 We observe that the first branch of the spectrum rests in the sector  $V < 1$ ,  
229 where  $\lambda_{1,2}$  are real numbers, and therefore, for large values of  $K$ , we have  
230  $\coth \lambda_{1,2} \rightarrow 1$  and the solution of (39) tends to the Rayleigh wave speed equation  
231 (28). Consequently, for this branch, SV modes cannot act as guiding curves, i.e.  
232 the spectrum branches do not follow any of the SV modes (32) (see [17, §4] for  
233 a different take on the concept of guiding curve). In contrast, for all the other  
234 branches of the Rayleigh-Lamb frequency spectrum, SV modes are guidelines  
235 in the short-wave high-frequency (SWHF) regime. This occurs because such  
236 branches rest in the sector  $1 < V < V_1$  where  $\lambda_1$  is purely imaginary and  $\lambda_2$  real;  
237 as  $K$  grows larger,  $\coth \lambda_1$  oscillates wildly unless (32) holds, while  $\coth \lambda_2 \rightarrow 1$ .  
238 Then, Eq.(39) is satisfied provided that  $s_2 \rightarrow 0$ , which occurs for  $V \rightarrow 1^+$ . We  
239 thus proved that a definite SWHF limit exists provided that the spectrum  
240 branches follow odd SV modes and their phase velocity asymptotes the shear  
241 bulk wave speed from above. A similar analysis reveals that, in the sector  
242  $V > V_1$ , P modes act as guiding curves.

243 We conclude that, when the wavelength becomes very small compared to the  
244 plate thickness, only the first spectrum branch is independent of the boundary  
245 pair and behaves like only one existed. We can then interpret SV (P) modes as  
246 the perturbation of shear (longitudinal) bulk waves which take into account the  
247 pair of boundaries.

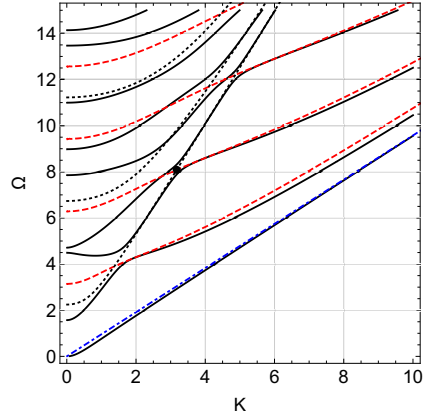


**Figure 6.** Frequency spectrum for antisymmetric waves (42) in a carbon epoxy-resin composite plate (solid black curves) superposed onto even SV (dashed, red) and odd P (dotted, black) mode spectra. A veering point (black dot) and the Rayleigh wave line spectrum (dash-dotted, blue) are also presented

248 We further emphasize that the concept of guiding curve is strictly related to  
 249 the idea of weak coupling in the sense developed in [1]. Indeed, for a weakly  
 250 coupled system, the spectrum branches quickly collapse onto partial waves  
 251 outside the close neighbourhood of the veering points.

252 The long-wave low-frequency (LWLF) approximation of the first symmetric  
 253 spectrum branch reveals that the system behaviour is equivalent to longitudinal  
 254 vibrations of a beam-plate with young modulus  $E_c$

$$E_c k^2 = \rho \omega^2.$$

### 255 *Antisymmetric waves*

256 Consideration of antisymmetric (flexural) waves demands taking the odd part  
 257 for  $\sigma_{yy}$  and the even part for  $\sigma_{xy}$  in Eqs.(35) and it gives the homogeneous  
 258 algebraic system

$$\mathbf{A}(K^2, \Omega^2) \begin{bmatrix} o_1 \\ o_2 \end{bmatrix} = \begin{bmatrix} 0 \\ 0 \end{bmatrix}, \quad (40)$$

where

$$\mathbf{A}(K^2, \Omega^2) = \begin{bmatrix} \zeta_{11} \sinh \lambda_1 & \zeta_{12} \sinh \lambda_2 \\ -i\zeta_{21} \cosh \lambda_1 & -i\zeta_{22} \cosh \lambda_2 \end{bmatrix}.$$

259 This matrix may be rewritten in hermitian form

$$\mathbf{A}_h(K^2, \Omega^2) = \begin{bmatrix} i\zeta_{11}\zeta_{21} \frac{\sinh \lambda_1}{\sinh \lambda_2} & i s_2 \\ -i s_2 & -i\zeta_{12}\zeta_{22} \frac{\cosh \lambda_2}{\cosh \lambda_1} \end{bmatrix}. \quad (41)$$

260 The corresponding dispersion relation  $d_o = 0$  is (cfr. [4, Eq.(8.1.59)])

$$d_o(K^2, \Omega^2) = s_1 \tanh \lambda_1 - s_2 \tanh \lambda_2. \quad (42)$$

261 The frequency spectrum for flexural waves in a carbon-epoxy plate is shown in  
 262 Fig.6. We observe that even SV modes are obtained through setting  $A_{11} = 0$   
 263 and odd P modes through putting  $A_{22} = 0$ . Once again, the first branch rests  
 264 in the sector  $V < 1$  and therefore it asymptotes Rayleigh waves in the SWHF  
 265 approximation. Branches in the sector  $1 < V < V_1$  are guided by SV modes in  
 266 the SWHF limit and their phase speed tends to the shear bulk wave speed from  
 267 above; the argument going as in the symmetric case.

The long-wave low-frequency (LWLF) approximation of the first flexural spectrum branch is given by

$$D_{11}k^4 - 2h\rho\omega^2 = 0, \quad D_{11} = E_c I_{11}, \quad I_{11} = \frac{2}{3}h^3,$$

268 corresponding to flexural vibrations of an orthotropic Kirchhoff beam-plate with  
 269 flexural rigidity  $D_{11}$  and second moment of inertia  $I_{11}$ .

## 270 Internal veering

271 In classical veering, as illustrated in [10], the dispersion relation emerges setting  
 272 to zero the determinant of an hermitian matrix whose off-diagonal terms  
 273 are small. Indeed, diagonal terms represent the dispersion relation of some  
 274 mechanically well-defined 1D systems, while off-diagonal terms are expression of  
 275 the coupling among these. The hermitian nature of the matrix comes from the  
 276 action-reaction principle. In classical veering, therefore, each system is clearly  
 277 identifiable at the beginning and likewise are its dispersion modes. Besides,  
 278 the position of each mechanical system is defined by its own displacement  
 279 degree of freedom. Veering brings a rotation of the polarization vector from  
 280 one system to the other. Rayleigh-Lamb dispersion curves exhibit a different  
 281 form of veering, which we name internal after the observation that it originates  
 282 from the interaction of SV and P partial waves. In case of internal veering, the

283 definition of the interacting modes is not so straightforward. Also, polarization  
284 rotation occurs differently.

### 285 *Symmetric waves*

286 We now describe the essential features of internal veering with respect to  
287 symmetric modes for a free plate. Veering occurs when even P and odd SV modes  
288 intersect, that is veering points are located by solving the pair of transcendental  
289 equations

$$S_{11} = S_{22} = 0. \quad (43)$$

290 This amounts to letting in turn  $e_2 = 0$  and then  $e_1 = 0$ . With respect to  
291 the terminology developed in [10], this has no correspondence to either the  
292 uncoupled blocked system or to the uncoupled disconnected system. Indeed, as  
293 already pointed out, P and SV modes emerge from considering Mindlin's micro-  
294 chain or lubricated wall boundary conditions. Therefore, the interacting systems  
295 share the same kinematical description but differ by the boundary conditions.  
296 The off-diagonal entries are coupling terms and they correspond to odd P and  
297 even SV modes. In the hermitian writing of Eq.(38), a form of action-reaction  
298 principle is preserved.

Let  $(K_0, \Omega_0)$  define the position of a veering point, i.e. it is a solution of  
(43). To fix ideas, we consider veering points on the line  $\Omega_0 = V_1 K_0$  as in Fig.5,  
which arise from the interaction between odd SV modes and the first P mode  
(i.e. bulk longitudinal waves  $m = 0$ ). We observe that this choice appears most  
unfavourable, for we are right at the branch point for  $\lambda_2$ .  $K_0$  may be simply  
obtained by solving Eq.(32) with  $V = V_1$  (for bulk longitudinal waves we have  
 $\Lambda_2(V_1) = 0$ )

$$K_0 \Lambda_1(V_1) = i \frac{1}{2} (1 + 2n) \pi, \quad n \in \mathbb{N},$$

299 and making use of Eq.(24), we get

$$K_0^2 = \frac{(\frac{1}{2} + n)^2 \pi^2}{4(1 + V_2^{-2})(V_1^2 - V_*^2)}. \quad (44)$$

300 We observe that  $K_0$  is real provided that  $V_* < V_1$ , as we already assumed in  
301 (21). Besides, it is easy to see that

$$dV = \frac{d\Omega}{K} - \frac{\Omega}{K^2} dK, \quad (45)$$

302 and when  $(K, \Omega)$  lies on a curve  $V = \text{const}$  we get

$$dV = 0 \Leftrightarrow V = V_g, \quad (46)$$

303 that is the phase velocity equals the group velocity. Expanding in Taylor series  
 304 the matrix  $\mathbf{S}_h$  about the veering point is possible, despite the branch point  
 305 singularity for the square root in  $\Lambda_2(V_1)$ , because, as already mentioned, the  
 306 dependence on the lambdas is really through their square, which is the reason  
 307 by which the sign of the lambdas is immaterial. Indeed we find, at leading order,

$$(\mathbf{S}_{h_0} + d\mathbf{S}_h)[K, \Omega, K_0, \Omega_0] = \begin{bmatrix} q_{11}dK + r_{11}d\Omega & p_{12} \\ p_{21} & q_{22}dK + r_{22}d\Omega \end{bmatrix}, \quad (47)$$

where, after tedious manipulations,

$$r_{11} = -(-1)^n \zeta_{11}(V_1) \zeta_{21}(V_1) \frac{d\Lambda_1}{dV}(V_1), \quad (48a)$$

$$r_{22} = -(-1)^n \frac{c_{12}}{c_{12} + c_{66}} \zeta_{12}(V_1) \left( \frac{d\Lambda_2^2}{dV}(V_1) - 2 \frac{c_{66}}{c_{12}} V_1 \right), \quad (48b)$$

308 and

$$p_{12} = -p_{21} = \imath s_2(V_1). \quad (49)$$

In (48b), the derivative of  $\Lambda_2^2$  appears that is bounded. Making use of Eqs.(24,27,32), we see that

$$\begin{aligned} \zeta_{11}(V_1) &= 1 - \frac{c_{66} c_{22} + c_{66}}{c_{12} c_{12} + c_{66}} (V_1^2 - V_*^2), \\ \zeta_{12}(V_1) &= 1, \\ \zeta_{21}(V_1) &= -\frac{c_{12}}{c_{12} + c_{66}} \sqrt{(1 + V_2^{-2}) (V_1^2 - V_*^2)} = -\frac{c_{12}}{c_{12} + c_{66}} \frac{(\frac{1}{2} + n)\pi}{K_0}, \end{aligned}$$

309 which are functions of  $V_1$  alone.

310 In general,  $dK$  and  $d\Omega$  are arbitrary quantities, however, when moving along  
 311 a SV/P partial wave, we have, respectively,

$$d(K\Lambda_{1,2}) = 0, \quad (50)$$

whence we get the connection  $d\Omega = V_{g1,2}dK$  that, substituted into the expansion for  $dS_{11}$  ( $dS_{22}$ ), yields the result

$$\frac{q_{ii}}{r_{ii}} = -V_{g_i}, \quad i \in \{1, 2\}.$$

We observe that  $dK^2 = 2KdK$  and  $d\Omega^2 = 2\Omega d\Omega$ , thus  $d\Omega^2/dK^2 = VV_g$  is the product of the phase and group velocities. Then, recalling that the dispersion relation is a transcendental function of  $K^2$  and  $\Omega^2$ , we prefer to write (cfr.[10, Eq.(16)])

$$(\mathbf{S}_{h0} + d\mathbf{S}_h) [K^2, \Omega^2, V_1] = \begin{bmatrix} \frac{r_{11}}{2\Omega_0} (d\Omega^2 - c_1^2 dK^2) & \imath s_2(V_1) \\ -\imath s_2(V_1) & \frac{r_{22}}{2\Omega_0} (d\Omega^2 - c_2^2 dK^2) \end{bmatrix}, \quad (51)$$

where, making use of Eq.(46) for  $c_2$ ,

$$c_1 = \sqrt{V_1 V_{g1}}, \quad c_2 = \sqrt{V_1 V_{g2}} = V_1. \quad (52)$$

Consequently, we deduce that, in the neighbourhood of a veering point and within a leading term Taylor approximation, the system behaves like a pair of interacting tout strings, whose wave speeds  $c_1$  and  $c_2$  are the geometric mean of the relevant phase and group velocities. In particular, for all the countable infinite number of veering points on the line  $V = V_1$ , the tout strings wave speeds are the same and therefore veering repeats itself periodically. In general, we can say that the frequency spectra of the even P and odd SV partial waves define the envelope of the wave speed field for a pair of tout strings whose properties are frequency dependent.

Letting

$$\Delta K = K^2 - K_0^2, \quad \Delta \Omega = \Omega^2 - \Omega_0^2,$$

we write the approximate dispersion relation (cfr.[10, Eq.(14)])

$$\Delta \Omega^2 - (c_1^2 + c_2^2)\Delta K \Delta \Omega + c_1^2 c_2^2 \Delta K^2 - 4\Omega_0^2 \eta^2 = 0, \quad (53)$$

with

$$\eta^2 = \frac{s_2(V_1)^2}{r_{11}r_{22}}. \quad (54)$$

The approximation (53) may be obtained directly operating a Taylor expansion of the dispersion relation (39) up to second order terms. The solution of Eq.(53)

332 provides two branches, named upper and lower,

$$\Delta\Omega = \frac{1}{2}(c_1^2 + c_2^2)\Delta K \left( 1 \pm \sqrt{1 - 4 \frac{c_1^2 c_2^2 - 4\Omega_0^2 \eta^2 / \Delta K^2}{(c_1^2 + c_2^2)^2}} \right). \quad (55)$$

333 It should be emphasized that the string model expansion (51) is consistent  
 334 inasmuch as  $\Omega - \Omega_0$  and  $K - K_0$  are small, so that a leading term approximation  
 335 is meaningful. Assuming  $\Omega - \Omega_0 \sim K - K_0 \sim \varepsilon \ll 1$ , we have, for the solution  
 336 set of Eq.(53),

$$4\Omega_0^2 \eta^2 \sim 4\Omega_0^2 [1 - (c_1^2 + c_2^2)V_1^{-1} + c_1^2 c_2^2 V_1^{-2}] \varepsilon,$$

337 where  $\sim$  stands for "same order as". Whence, using (52), we demand

$$\eta^2 \sim (V_{g_1} - 1) (V_1 - 1) \varepsilon,$$

338 which is independent of the veering point under consideration, i.e. independent  
 339 of  $n$ . Therefore, here we require  $\eta^2$  to be small while  $4\Omega_0^2 \eta^2$  may be, and generally  
 340 is, large. This approach is at variance with that developed in [10]. As an example,  
 341 for steel we have  $\eta^2 \approx 0.28125$  and for carbon-epoxy  $\eta^2 \approx 0.0163$ . The smallness  
 342 of  $\eta^2$  sets the size of neighbourhood where the tout string approximation is  
 343 meaningful, regardless of the veering point under scrutiny.

### 344 *Numerical results*

345 Fig.7 plots the simple approximation (55) for a carbon epoxy composite plate at  
 346 the veering point corresponding to the SV mode  $n = 1$ . The same approximation  
 347 is repeated in Fig.8 for the SV mode  $n = 3$  and, as anticipated, the same  
 348 behaviour is matched. In general, consideration of the leading term alone  
 349 (string model) appears surprisingly accurate, even in the large, inasmuch as the  
 350 spectrum branches are well represented (guided) by the corresponding partial  
 351 waves. For instance, moving along the lower branch in Fig.7, we veer from  
 352 longitudinal bulk waves (P mode  $m = 0$ ) to the SV mode  $n = 1$ . In contrast,  
 353 the upper branch is generally not well described by either partial wave until the  
 354 close neighbourhood of veering is reached. For this reason, the Taylor expansion  
 355 method, as here described, is doomed to provide poor accuracy there, no matter  
 356 how many terms in the expansion. The reason by which the spectrum is not  
 357 guided by the SV mode on reaching the veering point along the upper branch

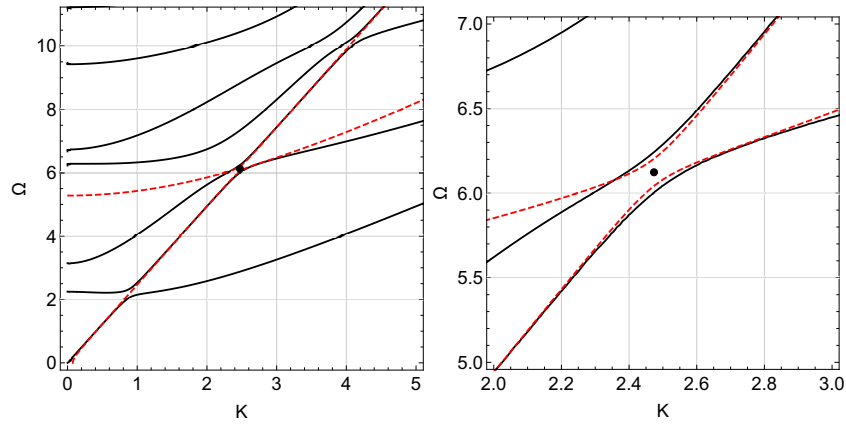


**Figure 7.** Approximation (55) near the veering point  $n = 1$  for a plate made of carbon epoxy composite (dashed, red) superposed onto the frequency spectrum of symmetric waves (solid, black)

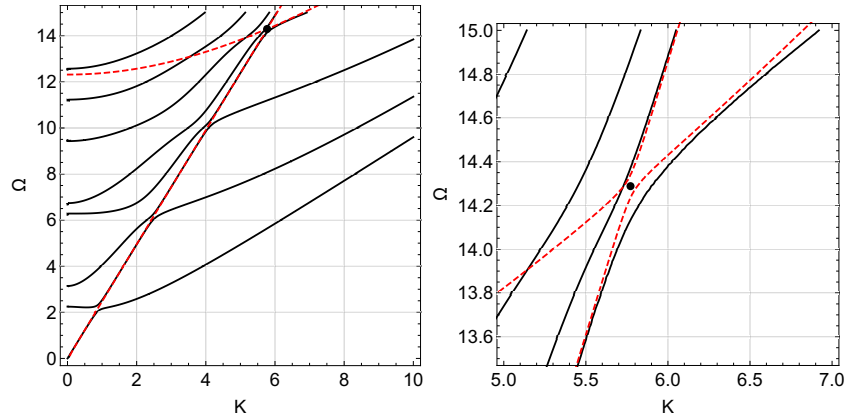


**Figure 8.** Approximation (55) near the veering point  $n = 3$  for a plate made of carbon epoxy composite (dashed, red) superposed onto the frequency spectrum of symmetric waves (solid, black)

358 may be ascribed to the presence of yet another veering point, so that the two  
 359 interact (see Fig.5). In fact, moving along the upper branch in Fig.7, we see that  
 360 the spectrum behaves in between a P and a SV mode until a point  $\bar{P}$  is reached  
 361 where  $S_{11} = S_{12} = 0$ . Beyond this point, the spectrum approaches the even P  
 362 mode  $m = 0$  and the approximation is excellent again. It should be emphasized  
 363 that this departure from the guiding curve is not possible in systems of 1D  
 364 elements, wherein dispersion is bound to a number of dispersion curves.

## 365 **Conclusions**

366 We analyse Rayleigh-Lamb (RL) modes in an orthorhombic layer with special  
367 emphasis on *veering*, that is a coupling phenomenon by which wave branches  
368 exchange their role in close proximity to their intersection point (the veering  
369 point). Physically, this amounts to destructive wave interference taking place  
370 at the veering point (that is a point of no propagation) and constructive  
371 interference occurring in its close neighbourhood. Interference occurs in such a  
372 way that the "emerging" wavemodes are swapped compared to the "incoming"  
373 modes. We first recall that RL modes are themselves originating from  
374 interference of *partial waves* (here named P and SV modes), which express waves  
375 complying with special boundary conditions allowing for no mode conversion.  
376 In this sense, partial waves appear "more fundamental" than RL modes, for it is  
377 precisely their combination through the boundary conditions which originates  
378 the latter. Indeed, this mechanism is apparent in the frequency spectrum of  
379 RL waves, wherein partial waves take up the role of guiding waves, in the  
380 sense that they bound the propagation curves. We show here that the same  
381 mechanism stands at the ground of veering. Indeed, veering points for symmetric  
382 (antisymmetric) RL modes corresponds to intersection points for even P/odd  
383 SV (odd P/even SV) partial waves. This situation can be compared with  
384 veering in two dimensional systems, wherein eigenmodes pertaining to either  
385 mechanical system (considered independent or uncoupled) interact by means  
386 of the coupling device. In the case of RL modes, asymptotic analysis reveals  
387 that interaction occurs in the form of a pair of tout strings whose wave speed  
388 are the geometric mean of the relevant wave phase and group velocities. An  
389 approximation dispersion relation is obtained whose range of validity depends  
390 on the strength of the coupling. Numerical results show that the quality of  
391 the approximation is good inasmuch as interaction among neighboring veering  
392 points does not occur. Indeed, this interaction weakens the role of partial waves  
393 as guiding waves.

## 394 **Acknowledgements**

395 AN acknowledges financial support from the MSCA RISE EU project 101008140  
396 "EffectFact".  
397 BE is grateful for financial support as visiting guest at Modena University.

---

398 **Declaration of Conflicting Interests**

399 The Authors declare that there is no conflict of interest

400 **References**

- 401 [1] E Manconi B Mace. Veering and strong coupling effects in structural  
402 dynamics. *Journal of Vibrations and Acoustics*, 139(2):021009–021009–10,  
403 2017.
- 404 [2] BA Auld. *Acoustic fields and waves in solids*. John Wiley & Sons, 1973.
- 405 [3] A Bhaskar. Waveguide modes in elastic rods. *Proceedings of the Royal  
406 Society of London. Series A: Mathematical, Physical and Engineering  
407 Sciences*, 459(2029):175–194, 2003.
- 408 [4] KF Graff. *Wave motion in elastic solids*. Dover Publishing, Inc, New York,  
409 1975.
- 410 [5] T Hussain and F Ahmad. Lamb modes with multiple zero-group velocity  
411 points in an orthotropic plate. *The Journal of the Acoustical Society of  
412 America*, 132(2):641–645, 2012.
- 413 [6] RM Jones. *Mechanics of composite materials*, volume 193. Scripta Book  
414 Company Washington, DC, 1975.
- 415 [7] J Kaplunov and A Nobili. Multi-parametric analysis of strongly  
416 inhomogeneous periodic waveguides with internal cutoff frequencies.  
417 *Mathematical Methods in the Applied Sciences*, 40(9):3381–3392, 2017.
- 418 [8] JD Kaplunov, LY Kossovitch, and EV Nolde. *Dynamics of thin walled  
419 elastic bodies*. Academic Press, 1998.
- 420 [9] SV Kuznetsov. Lamb waves in anisotropic plates. *Acoustical Physics*,  
421 60(1):95–103, 2014.
- 422 [10] BR Mace and E Manconi. Wave motion and dispersion phenomena:  
423 Veering, locking and strong coupling effects. *The Journal of the Acoustical  
424 Society of America*, 131(2):1015–1028, 2012.
- 425 [11] A Nobili. Asymptotically consistent size-dependent plate models based  
426 on the couple-stress theory with micro-inertia. *European Journal of  
427 Mechanics-A/Solids*, 89:104316, 2021.

- 
- 428 [12] A Nobili and DA Prikazchikov. Explicit formulation for the Rayleigh wave  
429 field induced by surface stresses in an orthorhombic half-plane. *European*  
430 *Journal of Mechanics-A/Solids*, 70:86–94, 2018.
- 431 [13] A Nobili, E Radi, and C Signorini. A new Rayleigh-like wave in guided  
432 propagation of antiplane waves in couple stress materials. *Proceedings of*  
433 *the Royal Society A*, 476(2235):20190822, 2020.
- 434 [14] AN Norris. Flexural waves on narrow plates. *The Journal of the Acoustical*  
435 *Society of America*, 113(5):2647–2658, 2003.
- 436 [15] D. Royer and E. Dieulesaint. Rayleigh wave velocity and displacement in  
437 orthorhombic, tetragonal, hexagonal, and cubic crystals. *The Journal of*  
438 *the Acoustical Society of America*, 76(5):1438–1444, 1984.
- 439 [16] D Royer and E Dieulesaint. Elastic waves in solids I: Free and guided  
440 propagation. *Springer-Verlag, New York*, 2000.
- 441 [17] LP Solie and BA Auld. Elastic waves in free anisotropic plates. *The Journal*  
442 *of the Acoustical Society of America*, 54(1):50–65, 1973.
- 443 [18] DJ Thompson, NS Ferguson, JW Yoo, and J Rohlfling. Structural waveguide  
444 behaviour of a beam–plate system. *Journal of sound and vibration*, 318(1-  
445 2):206–226, 2008.
- 446 [19] PE Tovstik. On the asymptotic nature of approximate models of  
447 beams, plates, and shells. *Vestnik St. Petersburg University: Mathematics*,  
448 40(3):188–192, 2007.
- 449 [20] PE Tovstik and TP Tovstik. Generalized Timoshenko-Reissner models  
450 for beams and plates, strongly heterogeneous in the thickness direction.  
451 *ZAMM-Journal of Applied Mathematics and Mechanics/Zeitschrift für*  
452 *Angewandte Mathematik und Mechanik*, 97(3):296–308, 2017.
- 453 [21] MN Zadeh and SV Sorokin. Comparison of waveguide properties of curved  
454 versus straight planar elastic layers. *Mechanics Research Communications*,  
455 47:61–68, 2013.